2021 American Control Conference (ACC)
New Orleans, USA, May 25-28, 2021

1D PDE Model for Thermal Dynamics in Fluid-Cooled Battery Packs: Numerical Methods and Sensor Placement

Dylan Kato[1], Scott J. Moura[1]

***Abstract*— This paper addresses the problem of modeling and estimating state dynamics in coupled battery and thermal cooling systems. We present a coupled diffusion-advection PDE model for fluid-cooled battery packs. A novel numerical method is proposed to simulate this PDE system. The technique is a monolithic integration of the method of characteristics and the Crank-Nicolson update scheme. The numerical scheme is validated with thermal energy conservation and shown to be conservative. We then leverage this numeric scheme to examine the optimal sensor placement problem. We formulate and solve the optimal sensor placement problem by designing the "C matrix" such that the mean square error of the Kalman filter state estimate is minimized.**

NOMENCLATURE

ΔT	Time discretization size [s]
ΔX	Spatial discretization size [m]
$\sigma(t)$	Cooling fluid velocity [$\frac{m}{s}$]
$D(x,t)$	Thermal diffusion coefficient [$\frac{m^2}{s}$]
$f_t(x,t)$	Partial derivative of f w.r.t. t
$f_x(x,t)$	Partial derivative of f w.r.t. x
$h(x,t,u)$	Heat generation in the pack [$\frac{K^\circ}{s}$]
$m(t)$	Process noise
$n(t)$	Sensor noise
N_t	Number of temporal discretization points
N_x	Number of spatial discretization points
$R(x,t)$	Lumped thermal resistance [$\frac{s}{1}$]
$U(t)$	Inlet temperature of cooling fluid [Kdeg]
$u(x,t)$	Temperature in the battery pack [K°]
$w(x,t)$	Temperature in the coolant [K°]
s	Characteristic parameter

I. INTRODUCTION

Understanding the temperature of battery cells is key to understanding their safety and aging behavior. A great deal of work has been put into understanding the health and safety of battery cells such as [1] [2] [3] [4] [5]. In studies of single cells, we often treat temperature as a measured output. However, in practice, batteries are assembled into packs which have design constraints on cost and space. This often makes it infeasible to measure the temperature of every cell in a battery pack. Instead, packs often have far fewer sensors than battery cells. With limited temperature information we still seek to model the temperature distribution throughout the pack. This allows us to understand how temperature heterogeneity impacts aging on cells that experience different conditions. Understanding heterogeneity in battery packs is one key motivation for developing thermal models for battery packs. Additionally, safety in battery packs is a big concern. Rapid detection of thermal runaway leads to better options for mitigation and higher levels of safety. Moreover, faster models that can be implemented online enable detection of thermal anomalies in battery packs with limited sensing.

A portion of the thermal modeling literature has focused on modeling battery pack thermal management systems using computational fluid dynamic models [6] [7]. These models capture the intricate complexities of fluid flow and heat transport. The models are also capable of explicitly capturing the geometry of the cooling system. The main drawback with computational fluid dynamic (CFD) models is that they are complex. Lower complexity models present two main advantages. First, simpler models decrease simulation run-time, allowing for more iterations in iterative design processes. Second, simpler models often allow for more rigorous control-theoretic analysis. Smyshlyaev et al. presents a 2D model of a thermal management system that homogenizes the cell, cooling channel, and pack material temperature states into coupled partial differential equations (PDE) – a simpler structure than computational fluid dynamic models [8]. Wolf et al. [9] considered sensor placement using eigen-mode decomposition using the model from [8].

A number of other models exist in the literature. Models like [10] and [11] model heat transfer in battery packs using two spatial dimensions like in [8]. Shi et al. models battery thermal management systems with lumped temperatures representing bulk estimates of thermal mass in regions of the system [12] . Another model from [13] and [14] models the temperature dynamics of several battery strings and the cooling channel by modeling the dynamics of each battery using a system of ODEs.

Given the state-of-art research described above, the contributions of this paper are: (i) a two-state PDE model of a battery pack and cooling channel thermal dynamics with one spatial dimension; (ii) a novel method of numerically solving the system; (iii) an optimal sensor placement framework based on the discretized PDE model.

Particularly, our paper builds on the state of the art models [8], [10], [11], [13] and [14] by presenting a PDE model for battery pack cooling systems. Our model has distinct advantages in that: (1) it has one spatial dimension, making it less computationally complex than CFD models, (2) using analysis of its PDE we can validate that the numerical scheme is conservative, which is important physically, (3) the model discretization is independent of the number of

[1]Dylan Kato, and Prof. Scott J. Moura are with the Energy, Controls and Applications Lab (eCAL), University of California, Berkeley, CA 94720, USA {dkkato, smoura}@berkeley.edu

cells in the pack.

We discretize our PDE model and impose our numerical solution scheme yielding a discrete time linear dynamical system. We demonstrate that this model allows us to solve complex engineering problems by performing optimal sensor placement in the context of linear systems. Particularly, we propose an optimization problem to design the state-to-output matrix, C, to minimize the mean square state estimation error. We solve this combinatorially to achieve the global optimum. This approach is enabled by the low dimension of our model since combinatorial approaches rapidly grow in required effort with increasing dimension.

The organization of this paper is as follows. In section II, we present the model, detailing the states, parameters, and inputs. In section III, we present a numerical method for simulating this model. In section IV, we derive and present an "Energy Based" validation metric for evaluating the numerical accuracy of the scheme. Finally, in section V, we pose and solve a sensor placement problem using this model.

II. PACK COOLING MODEL

Figure 1 provides a schematic overview of the model presented in this paper. The model has two states: one for the temperature distribution in the battery pack $u(x,t)$ and one for the tempearture distribution in the coolant $w(x,t)$. More complex models represent the cooling fluid as multi-dimensional (2D or 3D) and governed by the Navier-Stokes equations. This model reduces the complexity of the Navier-Stokes equation to the case of one dimensional, constant velocity flow. Likewise, the model of temperature across the battery pack is reduced to one dimension. Though some of the complexity is lost in this reduction, its structure allows us to solve combinatorial sensor placement problems, as we will show in Section V.

PDE Model equations

The following are the diffusion and advection equations that govern the system.

$$u_t(x,t) = D(x,t)u_{xx}(x,t) + h(x,t,u(x,t)) + \frac{1}{R(x,t)}(w(x,t) - u(x,t)) \quad (1)$$

$$w_t(x,t) = -\sigma(t)w_x(x,t) + \frac{1}{R(x,t)}(u(x,t) - w(x,t)) \quad (2)$$

Boundary conditions

Below are the boundary conditions. We use a Dirichlet boundary condition in the coolant PDE (4), which represents the temperature of the coolant at the inlet. The boundary condition in the pack (3) is Neumann, which physically corresponds to an adiabatic heat transfer process between the pack and its surrounding environment.

$$u_x(0,t) = u_x(1,t) = 0 \quad (3)$$

$$w(0,t) = U(t) \quad (4)$$

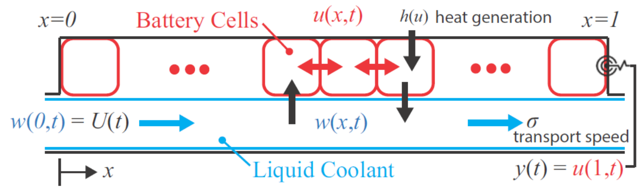

Fig. 1: this figure shows a schematic overview of the pack-coolant model

States

The model is physics-based and has two states: $u(x,t)$ and $w(x,t)$. State $u(x,t)$ is the temperature distribution across the pack. State $w(x,t)$ is the temperature distribution across the cooling fluid. The time-evolution of the spatial temperature distribution in the battery pack is governed by the Heat Equation, a second order PDE given by (1). The time-evolution of the spatial temperature distribution in the coolant is governed by the 1D advective transport equation, a first order PDE. These distributions are also coupled by a linear heat transfer term derived from Newton's law of heating (equivalently the Fourier law of heat transfer).

Parameters

The parameters of the model are $D(x,t)$ and $R(x,t)$. $D(x,t)$ is the thermal diffusion coefficient within the battery pack. $R(x,t)$ is the thermal resistance between the battery pack and the cooling fluid. These parameters can be tuned to simulate more complex battery pack shapes. The dependence of these parameters on x and t will be omitted from the notation henceforth for simplicity.

Inputs

The model has 3 inputs: $h(x,t,u)$, $U(t)$, and $\sigma(t)$. Source term $h(x,t,u)$ is the internal heat generation in the battery pack due to charging/discharge. The input $h(x,t,u)$ enters the system as an exogenous term in the battery pack PDE (1). Generally, $h(x,t,u)$ can be computed from a battery model and it would be a function of current imposed on the battery pack as well as temperature and other electrochemical states. Boundary input $U(t)$ is the temperature of the cooling fluid, and enters the system as a Dirichlet boundary condition at the inlet of the cooling fluid. In most systems, it makes sense to treat $U(t)$ as constant as if it were the temperature of the fluid coming from a reservoir with large thermal mass. Finally, $\sigma(t)$ is the transport speed of the cooling fluid. We restrict ourselves to the case of an incompressible fluid, and uniform cross-sectional area in the cooling fluid channel so $\sigma(t)$ is constant in x. For control problems using this model, one might pick $\sigma(t)$ as the chosen control. The dependence of $h(x,t,u)$ and $\sigma(x,t)$ on x and t will be omitted from the notation henceforth for notational simplicity.

III. NUMERICAL METHOD

To approximate solutions to these PDEs we use a numerical approach. The approach we developed combines the Crank-Nicolson and method of characteristics numerical schemes. Crank Nicolson is used to update the Diffusion Equation while Method of characteristics is used to simulate advection in the cooling fluid. We update $u(x,t)$ and $w(x,t)$ in one monolithic step, rather than updating each PDE state in alternation using the corresponding numerical method. This ensures the discrete solution satisfies both difference equations at each time step.

The Crank-Nicolson method is chosen for equation (1) because this method is unconditionally stable in the linear, uncoupled case. The method of characteristics is used for (2) because we found empirically that this method, when applied to the coupled system, was stable for larger Courant number ($\frac{\sigma * \Delta t}{\Delta x}$) than some other standard methods that approximate $\frac{\partial w}{\partial x}$ using Euler differences (ex. Upwind scheme, Lax-Wendroff).

Notational note

We use the standard numerical methods notation to denote the value of the states along the discretization lattice:

$$u_j^i = u(j\Delta X, i\Delta T) \tag{5}$$

$$w_j^i = w(j\Delta X, i\Delta T) \tag{6}$$

With this notation, i and j index a point on the discretized lattice. They take on values from discrete sets: $i \in [0, N_t] \cap \mathbb{Z}$ and $j \in [0, N_x] \cap \mathbb{Z}$ where N_t and N_x are the number of lattice points in the t and x dimensions respectively.

Crank-Nicolson

Equation (1) is discretized according to the Crank-Nicolson scheme. This scheme approximates the time derivative as the Euler central difference about $(j\Delta X, (i+\frac{1}{2})\Delta T)$ with step size $\frac{1}{2}\Delta T$. We approximate the spatial derivatives as the average between the second order central difference at $(j\Delta X, i\Delta T)$ and $(j\Delta X, (i+1)\Delta T)$. The derivative free terms are also averaged between $(j\Delta X, i\Delta T)$ and $(j\Delta X, (i+1)\Delta T)$ resulting in the following implicit scheme in the notation given by (5) and (6).

$$\begin{aligned}\frac{u_j^{i+1} - u_j^i}{\Delta T} =& \frac{D}{2\Delta X^2}[((u_{j-1}^{i+1} - 2u_j^{i+1} + u_{j+1}^{i+1})) \\ &+ ((u_{j-1}^i - 2u_j^i + u_{j+1}^i))] \\ &+ \frac{1}{2}(h(u_j^{i+1}) + h(u_j^i)) \\ &+ \frac{1}{2R}((w_j^i - u_j^i) + (w_j^{i+1} - u_j^{i+1}))\end{aligned} \tag{7}$$

Method of Characteristics

The method of characteristics is a general method for solving partial differential equations, particularly first-order PDEs. In the case of the linear advection equation, this method is analogous to taking a Lagrangian reference frame. That is, we look at the function $w(x,t)$ along lines parametrized as $(x(s), t(s))$=$(\sigma s, s)$. We call these parametric lines "characteristic curves." Under this change of variables, when we differentiate with respect to s we have that:

$$\begin{aligned}\frac{d}{ds}w(x(s),t(s)) = & \frac{\partial}{\partial x}w(x(s),t(s)) * \frac{d}{ds}x(s) \\ &+ \frac{\partial}{\partial t}w(x(s),t(s)) * \frac{d}{ds}t(s)\end{aligned}$$

Substituting the PDE (2) and evaluating $\frac{d}{ds}t(s) = 1$ and $\frac{d}{ds}x(s) = \sigma$ gives:

$$\begin{aligned}\frac{d}{ds}w(x(s),t(s)) =& \frac{\partial}{\partial x}w(x(s),t(s)) * \sigma \\ &- \sigma\frac{\partial}{\partial x}w(x(s),t(s)) \\ &+ \frac{1}{R}[u(x(s),t(s)) \\ &- w(x(s),t(s)))]\end{aligned}$$

The first two terms cancel to yield an ODE in s:

$$\begin{aligned}\frac{d}{ds}w(x(s),t(s)) =& \frac{1}{R}[u(x(s),t(s)) \\ &- w(x(s),t(s)))]\end{aligned}$$

Finally we can approximate the derivatives along s using Euler backwards difference for the time derivative. Similar to the Crank-Nicholson method, we obtain an implicit scheme by taking the average of the right hand side terms. Setting $\Delta T = \Delta S$, this gives us the update along the characteristic:

$$\begin{aligned}\frac{w_j^{i+1} - w(j\Delta X - \sigma\Delta T, i\Delta T)}{\Delta T} =& \frac{1}{2R}[(u_j^{i+1} - w_j^{i+1}) \\ &+ (u(j\Delta X - \sigma\Delta T, i\Delta T) \\ &- w(j\Delta X - \sigma\Delta T, i\Delta T))]\end{aligned} \tag{8}$$

This scheme works with our discretization $\Delta X, \Delta T$ provided $(j\Delta X - \sigma\Delta T, i\Delta T)$ lies on the lattice of discretization points. This is the case only when ΔX divides $\sigma\Delta T$. However, because we do not want to be constrained to discretizations where ΔX divides $\sigma\Delta T$ we approximate the values at the points $(j\Delta X - \sigma\Delta T, i\Delta T)$ via interpolation.

Interpolation

We interpolate the value of our state along the characteristic using linear interpolation between the two nearest neighbors of the point $j\Delta X - \sigma\Delta T$. Assuming that we chose ΔT and ΔX so that they satisfy $\Delta X \geq \sigma\Delta T$ the interpolation can be written as:

$$w(j\Delta X - \sigma\Delta T, i\Delta T) = \lambda w_j^i + (1-\lambda)w_{j-1}^i \tag{9}$$

$$\text{where} \quad \lambda = \frac{\Delta X - \sigma\Delta T}{\Delta X}$$

By coupling the method of characteristics update with this interpolation we derive an implicit update relation between function values on the discretization lattice.

Boundary Equations

Finally, we have the following equations for the boundary. In the cooling fluid, $w(x,t)$, we have a Dirichlet boundary condition which we implement as.

$$w_0^i = U(i\Delta T) \tag{10}$$

To handle the Neumann boundary conditions in the pack we introduce "ghost nodes." These are points one spatial step outside of the domain (i.e. $(0 - \Delta X, t)$ and $(1 + \Delta X, t)$) where we allow the function $u(x,t)$ to have value. We then assert at the left boundary that:

$$u_{-1}^i = u_1^i \tag{11}$$

This assures that the central difference at the left boundary, given by $\frac{u_1^i - u_{-1}^i}{\Delta X}$, is zero. We then do the same for the right boundary to complete the boundary conditions. This ghost node approach is convenient in that we can use the second order central difference scheme to approximate diffusion throughout the entire domain, rather than having to change the numerical scheme for the points at the edge of the domain.

Matrix form

Note that for each spatial discretization point $(i\Delta X, t)$ we have two state values $u(i\Delta X, t)$ and $w(i\Delta X, t)$. With the addition of the 2 ghost nodes for the battery pack state, we have a total of $2N_x + 2$ discrete states for each time step. Counting the equations, (7) gives N_x equations. Equations (8) combined with (9) gives $N_x - 1$ more. The boundary conditions (10) and (11) give 1 and 2 more equations respectively. This gives us a total of $2N_x + 2$ unknowns constrained by $2N_x + 2$ equations in total. This can be compactly written into matrix form:

$$A^+ z(i + \Delta T) - \frac{1}{2} H(z(i + \Delta T)) = Az(i) + \frac{1}{2} H(z(i)) \tag{12}$$

Here $z(i)$ is a column vector that holds the values of the states u_j^i and w_j^i for $j \in [-1, N_x + 1] \cap \mathbb{Z}$ at our current time step i. Note $z(i)$ holds the ghost nodes u_{-1}^i and $u_{N_x+1}^i$. The function $H(z)$ applies $h(x)$ from (1) elementwise to the elements of z corresponding to the battery pack temperature states $u(x,t)_j^i$ for $j \in [0, N_x] \cap \mathbb{Z}$ and is zero for states corresponding to the cooling fluid temperature and the "ghost nodes". Matrices A^+ and A contain the coefficients of the states from the Crank-Nicolson (7) and method of characteristics (8) updates. The interpolation step (9) is included in the method of characteristics rows of A. There are also 2 rows in these matrices that correspond to the "ghost node" equations (11).

The resulting scheme is implicit. Further, all the terms in the method of characteristics, interpolation, boundary conditions, and Crank-Nicolson equations are linear in the states with the exception of term $H(x)$. Since (12) is implicit, the states at the next time step are solutions to a system of equations, rather than given in closed form by a formula.

In the nonlinear case, we can use the Newton-Raphson method to find the points that solve this implicit equation at each time step. In the linear case, these implicit equations reduce to a system of linear equations as detailed in Section V. This means that calculating the next time step is just a matter of matrix multiplication rather than using Newton-Raphson.

IV. Energy Based Validation

To validate our numerical scheme and simulations we use an analysis of the total thermal energy flow to ensure that the numerical method maintains certain properties of the original PDE. We begin by defining the energy function:

$$\begin{aligned} E(t) = &\int_0^1 u(x,t)dx \\ &- \int_0^t \int_0^1 \frac{1}{R(x,\tau)}(w(x,\tau) - u(x,\tau)) + h(x,\tau,u)dxd\tau \end{aligned} \tag{13}$$

We label the terms of this equation according to physical meaning

Heat absorbed from coolant:

$$-\int_0^T \int_0^1 \frac{1}{R(x,t)}(w(x,t) - u(x,t))dxdt$$

Heat in pack:

$$\int_0^1 u(x,T)dx$$

Heat influx:

$$-\int_0^T \int_0^1 h(x,t,u)dxdt$$

Theorem 1. *Assume the states $u(x,t)$ and $w(x,t)$ obey the PDEs (1), (2), (3), (4). Then $E(t)$ is constant.*

Proof First, we take the derivative of $E(t)$ with respect to t using Lebnitz integral rule:

$$\begin{aligned} \frac{d}{dt}E(t) = &\int_0^1 u_t(x,t)dx \\ &- \int_0^1 \frac{1}{R(x,t)}(w(x,t) - u(x,t)) + h(x,t,u)dx \end{aligned}$$

We can now combine the integrands and substitute our governing equation (1) yielding:

$$\frac{d}{dt}E(t) = \int_0^1 u_{xx}(x,t)dx \tag{14}$$

Evaluating the right hand side of (14) and applying the Neumann boundary conditions (3) gives.

$$\begin{aligned} \frac{d}{dt}E(t) &= u_x(x,t)|_{x=0}^{x=1} \\ &= u_x(1,t) - u_x(0,t) \\ &= 0 \end{aligned} \tag{15}$$

Since $\frac{d}{dt}E(t) = 0$ we have shown that $E(t)$ is constant. Thus we can validate the simulation by approximating $E(T)$ via numerical integration and verifying it is constant.

In Fig. 2 we plot $E(t)$ as well as each term of (13). We refer to $E(t)$ as the Total System Heat and it is shown to be constant. This illustrates that the proposed numerical scheme is conservative, in the sense of conserving thermal energy. This result improves our confidence that the numerical solution is consistent with the pde.

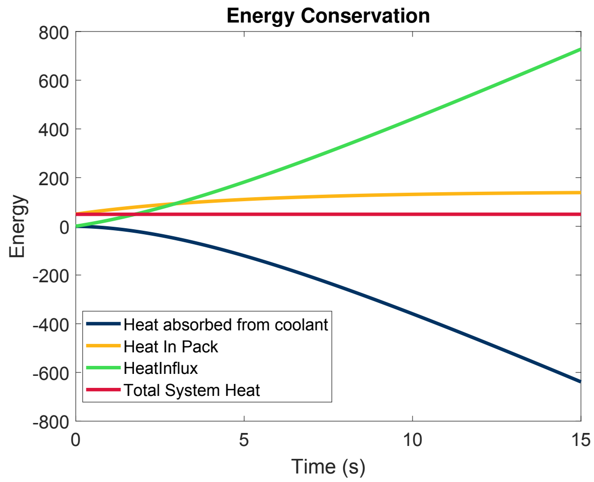

Fig. 2: Energy conservation analysis. Note that the red line representing the total energy $E(t)$ remains constant, demonstrating that the proposed numerical scheme is conservative.

V. Sensor Placement

A key advantage of the efficient and accurate numerical scheme above is that it enables design, control, and estimation tasks that involve iterative optimization. In this section, we leverage the propose numerical scheme to optimally place temperature sensors in the battery pack system.

Nonlinearity:

For the sensor placement problem we focus on a particular form of $H(u)$. Particularly one of the form $h(t,x,u) = \alpha(x,t) * u(x)$ where $\alpha(x,t)$ is a constant with respect to u. Since this form is linear in u, we can write it as a constant matrix acting on the state vector i.e. $H(z) = Fz$. Substituting this into (12) gives

$$(A^+ - \frac{1}{2}F)z(k+1) = (A + \frac{1}{2}F)z(k) \tag{16}$$

In the case that $(A^+ - \frac{1}{2}F)$ is invertible, we can write the implicit update in an explicit form

$$z(k+1) = \left(A^+ - \frac{1}{2}F\right)^{-1}\left(A + \frac{1}{2}F\right)z(k) \tag{17}$$

This transforms the update equations into a discrete time linear system. Note we have replaced the time index with k, for notational consistency with the literature.

Now, consider that we have process and sensor noise corrupting the state evolution and measurement respectively. Then our system of equations becomes:

$$z(k+1) = Az(k) + m(k) \tag{18}$$

$$y(k) = Cz(k) + n(k) \tag{19}$$

where $A = (A^+ - 0.5F)^{-1}(A + 0.5F)$. $m(k)$ is the process noise and $n(k)$ is the measurement noise. Both noise terms are assumed to be Gaussian with zero mean and respective covariances M and N. Additionally, we are constrained to choose C with a form where each row contains exactly one entry equal to one, corresponding to placing a sensor at that location in the battery pack or cooling fluid.

We are interested in investigating the case where the internal heat generation overwhelms the heat removal by the cooling fluid, resulting in thermal runaway [15]. In cases like this, state monitoring is crucial for mitigation and safety. To construct this case, we take F to destabilize the system by choosing F large enough so that the spectral radius of the system matrix $A = (A^+ - 0.5F)^{-1}(A + 0.5F)$ is greater than one.

Next we use the discrete-time Kalman filter to estimate the states of this system:

$$\hat{z}_{k|k-1} = A\hat{z}_{k-1|k-1} \tag{20}$$

$$\Sigma_{k|k-1} = A\Sigma_{k-1|k-1}A^T \tag{21}$$

$$\hat{y}_k = C\hat{z}_{k|k-1} \tag{22}$$

$$L_k = \Sigma_{k|k-1}C^T[C\Sigma_{k|k-1}C^T + N]^-1 \tag{23}$$

$$\hat{z}_{k|k} = \hat{z}_{k|k-1} + L_k[y_k - \hat{y}_k] \tag{24}$$

$$\Sigma_{k|k} = \Sigma_{k|k-1} - L_k[C\Sigma_{k|k-1}C^T + N]L_k^T \tag{25}$$

Note that the Kalman filter equations not only propagate the state estimates $\hat{x}_{k|k}$ but also the covariance $\Sigma_{k|k}$ of the state estimates according to equations (21),(23),(25).

Define the state estimation error to be: $\tilde{z}_k = z_k - \hat{z}_{k|k}$. Then the mean square of the estimation error can be computed from the trace of the covariance matrix $\Sigma_{k|k}$. Namely:

$$\mathbb{E}[\tilde{z}_k^T\tilde{z}_k] = \text{Tr}\left(\Sigma_{k|k}\right) \tag{26}$$

Taking the sum $\Sigma_{k=1}^{N_t}\text{Tr}\left(\Sigma_{k|k}\right)$ gives a measurement of the transient mean square state estimate error, a quantity we seek to minimize. To accomplish this, we seek to design measurement matrix C so that this quantity is minimized. This leads to the following combinatorial optimization problem in the decision variable C:

$$\min_C \quad \Sigma_{k=1}^{N_t}\text{Tr}\left(\Sigma_{k|k}\right) \tag{27}$$

$$\text{s.to}: \quad \Sigma_{k|k-1} = A\Sigma_{k-1|k-1}A^T + W \tag{28}$$

$$L_k = \Sigma_{k|k-1}C^T[C\Sigma_{k|k-1}C^T + N]^-1 \tag{29}$$

$$\Sigma_{k|k} = \Sigma_{k|k-1} - L_k[C\Sigma_{k|k-1}C^T + N]L_k^T \tag{30}$$

$$C_{ij} \in \{1, 0\} \tag{31}$$

$$\sum_{j=1}^{2N_x+2} C_{ij} = 1; \forall i \in \{1, 2, ...N_{sensors}\} \tag{32}$$

The constraints (28), (29), and (30) are the dynamics of the Kalman filter. The constraints eq.(31) and eq.(32) restrict C to the specified form.

We solved this problem by enumerating over all possible C matrices for the case of 3 sensors. A projection of the resulting objective function is shown in Fig. 3 when fixing one sensor at the outlet of the cooling channel. As can be seen, the resulting objective surface is non-convex and nonlinear. Fig. 4 show the resulting state estimate error when using optimal sensor placement. The state estimate error $\tilde{z}$ converges to 0 much more quickly when the sensors are placed using the above optimization.

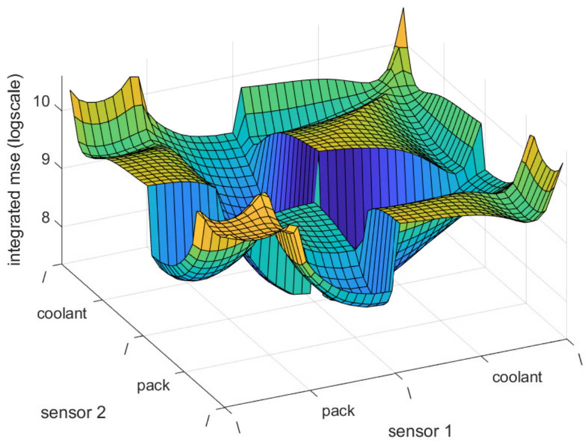

Fig. 3: This shows the cumulative mse when we place one sensor at the outlet of the cooling channel and allow the other two sensors to vary position throughout the coolant and the battery pack

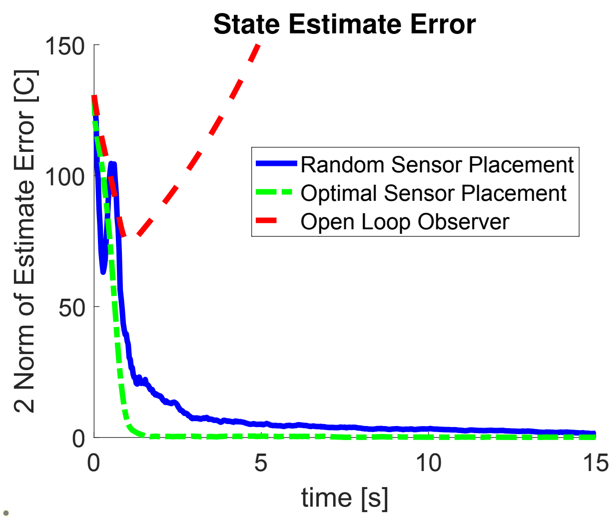

Fig. 4: This figure compares the transient behavior of state estimate for the case with 3 optimally places sensors, 3 randomly placed sensors, and 0 sensors (open loop observer)

VI. Conclusions

In this paper, we propose a one-dimensional PDE model for battery packs with fluid cooling. We provide numerical methods for simulating this model and an energy based validation of this model. Finally, we use the model to solve a sensor placement problem.

Potential extensions of this work involve solving control problems with this model. Although we validated the numerical scheme's consistency with the PDEs, validation to CFD models could give better insight into this model's accuracy. Better yet, experimental validation of the model would help us further understand the extent of this model's consistency with real-world battery cooling systems. Additionally, model-to-model comparison to CFD or experimental data would present interesting problems in estimating the diffusion and resistance parameters of the model.

Acknowledgment

This material is based upon work supported by the National Science Foundation Graduate Research Fellowship Program under Grant No. DGE 1752814. Any opinions, findings, and conclusions or recommendations expressed in this material are those of the author(s) and do not necessarily reflect the views of the National Science Foundation.

References

[1] D. Zhang, S. Dey, H. E. Perez, and S. J. Moura, "Remaining useful life estimation of lithium-ion batteries based on thermal dynamics," in *American Control Conference (ACC), 2017*. IEEE, 2017, pp. 4042–4047.

[2] S. J. Moura, J. L. Stein, and H. K. Fathy, "Battery-health conscious power management in plug-in hybrid electric vehicles via electrochemical modeling and stochastic control," *IEEE Transactions on Control Systems Technology*, vol. 21, no. 3, pp. 679–694, 2013.

[3] T. M. Bandhauer, S. Garimella, and T. F. Fuller, "A critical review of thermal issues in lithium-ion batteries," *Journal of the Electrochemical Society*, vol. 158, no. 3, p. R1, 2011.

[4] S. J. Moura, N. Chaturvedi, and M. Krstic, "Adaptive pde observer for battery soc/soh estimation," in *2012 ASME Dynamic Systems and Control Conference*, 2012.

[5] S. Dey, Z. A. Biron, S. Tatipamula, N. Das, S. Mohon, B. Ayalew, and P. Pisu, "Model-based real-time thermal fault diagnosis of lithium-ion batteries," *Control Engineering Practice*, vol. 56, pp. 37–48, 2016.

[6] K. E. Thomas, J. Newman, and R. M. Darling, "Mathematical modeling of lithium batteries," in *Advances in lithium-ion batteries*. Springer, 2002, pp. 345–392.

[7] T. Wang, K. Tseng, J. Zhao, and Z. Wei, "Thermal investigation of lithium-ion battery module with different cell arrangement structures and forced air-cooling strategies," *Applied energy*, vol. 134, pp. 229–238, 2014.

[8] A. Smyshlyaev, M. Krstic, N. Chaturvedi, J. Ahmed, and A. Kojic, "Pde model for thermal dynamics of a large li-ion battery pack," in *Proceedings of the 2011 American Control Conference*. IEEE, 2011, pp. 959–964.

[9] P. Wolf, S. Moura, and M. Krstic, "On optimizing sensor placement for spatio-temporal temperature estimation in large battery packs," in *2012 IEEE 51st IEEE Conference on Decision and Control (CDC)*. IEEE, 2012, pp. 973–978.

[10] Y. Chen and J. W. Evans, "Thermal analysis of lithium polymer electrolyte batteries by a two dimensional model—thermal behaviour and design optimization," *Electrochimica acta*, vol. 39, no. 4, pp. 517–526, 1994.

[11] G. Karimi and X. Li, "Thermal management of lithium-ion batteries for electric vehicles," *International Journal of Energy Research*, vol. 37, no. 1, pp. 13–24, 2013.

[12] Y. Shi, K. Smith, E. Wood, and A. Pesaran, "A multi-node thermal system model for lithium-ion battery packs," in *2015 American Control Conference (ACC)*. IEEE, 2015, pp. 723–727.

[13] X. Lin, H. Fu, H. E. Perez, J. B. Siege, A. G. Stefanopoulou, Y. Ding, and M. P. Castanier, "Parameterization and observability analysis of scalable battery clusters for onboard thermal management," *Oil & Gas Science and Technology–Revue d'IFP Energies nouvelles*, vol. 68, no. 1, pp. 165–178, 2013.

[14] C. Park and A. K. Jaura, "Dynamic thermal model of li-ion battery for predictive behavior in hybrid and fuel cell vehicles," SAE Technical Paper, Tech. Rep., 2003.

[15] Q. Wang, B. Mao, S. I. Stoliarov, and J. Sun, "A review of lithium ion battery failure mechanisms and fire prevention strategies," *Progress in Energy and Combustion Science*, vol. 73, pp. 95–131, 2019.